Structure and Dynamics of Water Confined in Single-Wall Nanotubes

Tanin Nanok,[†,‡,§] Nongnuch Artrith,[†,‡,∥] Piboon Pantu,[†,‡] Philippe A. Bopp,[⊥] and Jumras Limtrakul*[,†,‡]

Laboratory for Computational and Applied Chemistry, Department of Chemistry, Faculty of Science and Center of Nanotechnology, Kasetsart University, Bangkok 10900, Thailand, NANOTEC Center of Excellence, National Nanotechnology Center, Kasetsart University, Bangkok 10900, Thailand, and Department of Chemistry, Université Bordeaux 1, 351 Cours de la Libération, Building A12, F-33405 Talence cedex, France

Received: October 7, 2008; Revised Manuscript Received: November 28, 2008

The structure and dynamics of water confined in model single-wall carbon- and boron-nitride nanotubes (called SWCNT and SWBNNT, respectively) of different diameters have been investigated by molecular dynamics (MD) simulations at room temperature. The simulations were performed on periodically extended nanotubes filled with an amount of water that was determined by soaking a section of the nanotube in a water box in an *NpT* simulation (1 atm, 298 K). All MD production simulations were performed in the canonical (*NVT*) ensemble at a temperature of 298 K. Water was described by the extended simple point charge (SPC/E) model. The wall−water interactions were varied, within reasonable limits, to study the effect of a modified hydrophobicity of the pore walls. We report distribution functions for the water in the tubes in spherical and cylindrical coordinates and then look at the single-molecule dynamics, in particular self-diffusion. While this motion is slowed down in narrow tubes, in keeping with previous findings (Liu et al. *J. Chem. Phys.* **2005**, *123*, 234701−234707; Liu and Wang. *Phys. Rev.* **2005**, *72*, 085420/1−085420/4; Liu et al. *Langmuir* **2005**, *21*, 12025−12030) bulk-water like self-diffusion coefficients are found in wider tubes, more or less independently of the wall−water interaction. There may, however, be an anomaly in the self-diffusion for the SWBNNT.

I. Introduction

Carbon nanotubes (CNTs) have gained recognition as prominent building blocks of nanomaterials; they are used in a variety of nanotechnology applications due to their exceptional mechanical and electrical properties.[1,2] The transport of molecules in these nanoporous media could also exhibit interesting characteristics, different from the ones of transport in ordinary bulk media, since the interactions between the pore wall and the molecules become rather strong when the dimensions of the pore approach the size of the transported molecule. Although the mechanical and electrical properties of CNTs can be measured explicitly in experiments,[3] the understanding of the transport and conduction mechanisms through their pores is still incomplete. This is partly due to the difficulty of preparing CNTs with uniform pore sizes and distributions and of tracing the diffusive behavior inside. Computational studies thus play an important role in the interpretation of experimental data and provide predictive information on molecular transport through nanopores.

Because of the simplicity and hydrophobicity of their interior, CNTs are recognized as promising prototype models. They are frequently used as models for systems such as water transport in aquaporin water channels,[4] water migration in xylem vessels of plants,[5] the delivery of beneficial molecules to target cells[6−8] and other biological nanofluidic systems.

A previous molecular dynamics (MD) simulation study[9] on water conduction through the channel of single-walled carbon nanotubes (SWCNTs) showed that under normal conditions of pressure and temperature the filling of an empty (6,6)-CNT channel (8.1 Å in diameter and 13.4 Å in length) with water takes place within a few ten picoseconds. The channel then remained filled during the entire simulation time of 66 ns. The water molecules constrained in such a narrow space form a one-dimensionally ordered hydrogen-bond network that is not observed in bulk water. It was shown[10] that the channel occupancy and conductivity are dramatically decreased by a reduction of the attractive nanotube−water interactions. A 25% reduction leads to fluctuations between filled and empty sections in the tube and a 40% reduction to an emptying of the CNT channel.[9] This filling and conducting behavior has also been observed in an isoelectronic nanotube (a subnanometer boron nitride nanotube (BNNT)[11]) and other hydrophobic nanopores.[12,13]

Recently, several MD simulation studies have been performed on the diameter dependence of the CNT hydration. It was, for example, found that water confined in a critical-size armchair-(9,9) CNT can undergo a transition into a state having an ice-like mobility with an average number of hydrogen bonds close to that in bulk water under ambient temperature and pressure.[14] Unusual features, not seen in bulk ice, can also be observed with other CNT diameters under conditions of high water densities[15] and extremely high axial pressures (50 Mpa to 500 Mpa).[16] The radial distribution functions reveal highly ordered layered water structures in this case. For the dynamic properties, the radial and axial diffusivities of water encapsulated in SWCNTs are smaller than those of bulk water; both components

* Corresponding author. E-mail: fscijrl@ku.ac.th.
† Faculty of Science, Kasetsart University.
‡ NANOTEC Center of Excellence, Kasetsart University.
§ Present address: Institut für theoretische Physik, Universität Leipzig, Vor dem Hospitaltore, D-04103 Leipzig, Germany.
∥ Present address: Lehrstuhl für Theoretische Chemie, Ruhr-Universität Bochum, D-44780 Bochum, Germany.
⊥ Université Bordeaux 1.

10.1021/jp8088676 CCC: $40.75
Published on Web 12/30/2008

TABLE 1: Details for the MD Simulation Runs of Water in Carbon- and Boron-Nitride Nanotubes in This Work[a]

tube	effective inner diameter (Å)	no. of water molecules	simulation time (ns)
(9,9)-nanotubes	8.86	77	4
(10,10)-nanotubes	10.22	102	4
(12,12)-nanotubes	12.92	162	1
(14,14)-nanotubes	15.62	237	1
(16,16)-nanotubes	18.34	327	1
(20,20)-nanotubes	23.74	547	1

[a] The length is 36.89 Å in all cases.

decrease as the diameter of the SWCNTs decreases.[15,17,18] In other tubes with similar diameters, the flow of water was found to be strongly influenced by the hydrophilicity of the wall.[19,20] The strong interfacial water−nanotube attraction causes a significant reduction of the water flow rate.

Even though the structure and dynamics of water confined in SWCNTs have been extensively studied by MD simulations, most efforts have been directed toward small diameter tubes, in which the characteristics of bulk water cannot be attained even at the tube center. Thus, a more comprehensive understanding of the structural and dynamic properties of water confined in larger diameter SWCNTs seems to be desirable. Here, we study tubes with effective diameters (see below) between 8.86 to 23.74 Å and report on the influences of the attractive interactions between the wall and the confined water at an average density of 1.0 g/cm^3 under ambient conditions.

In the next section, the models and simulation details will be presented. Then, we will investigate the structure of the water in the tubes in terms of radial and cylindrical distribution functions. A study of the self-diffusion will then be presented.

II. Models and Simulation Details

The armchair type SWCNTs considered in this study are modeled as rigid networks of uncharged Lennard-Jones (LJ) carbon atoms with C−C bond distances of 1.42 Å and a fixed nanotube length of 36.89 Å. To study the diameter dependence of the structural and dynamic properties of the confined water, the "effective diameter" (i.e., the diameter after excluding the van der Waals radius of a C atom, 1.70 Å) is varied from 8.86 to 23.74 Å, corresponding to the (*m*,*m*)-armchair SWCNTs with $m = 9$, 10, 12, 14, 16 and 20, respectively. m is an integer in the chiral vector $\mathbf{A} = m\mathbf{a}_1 + m\mathbf{a}_2$ of the hexagonal honeycomb

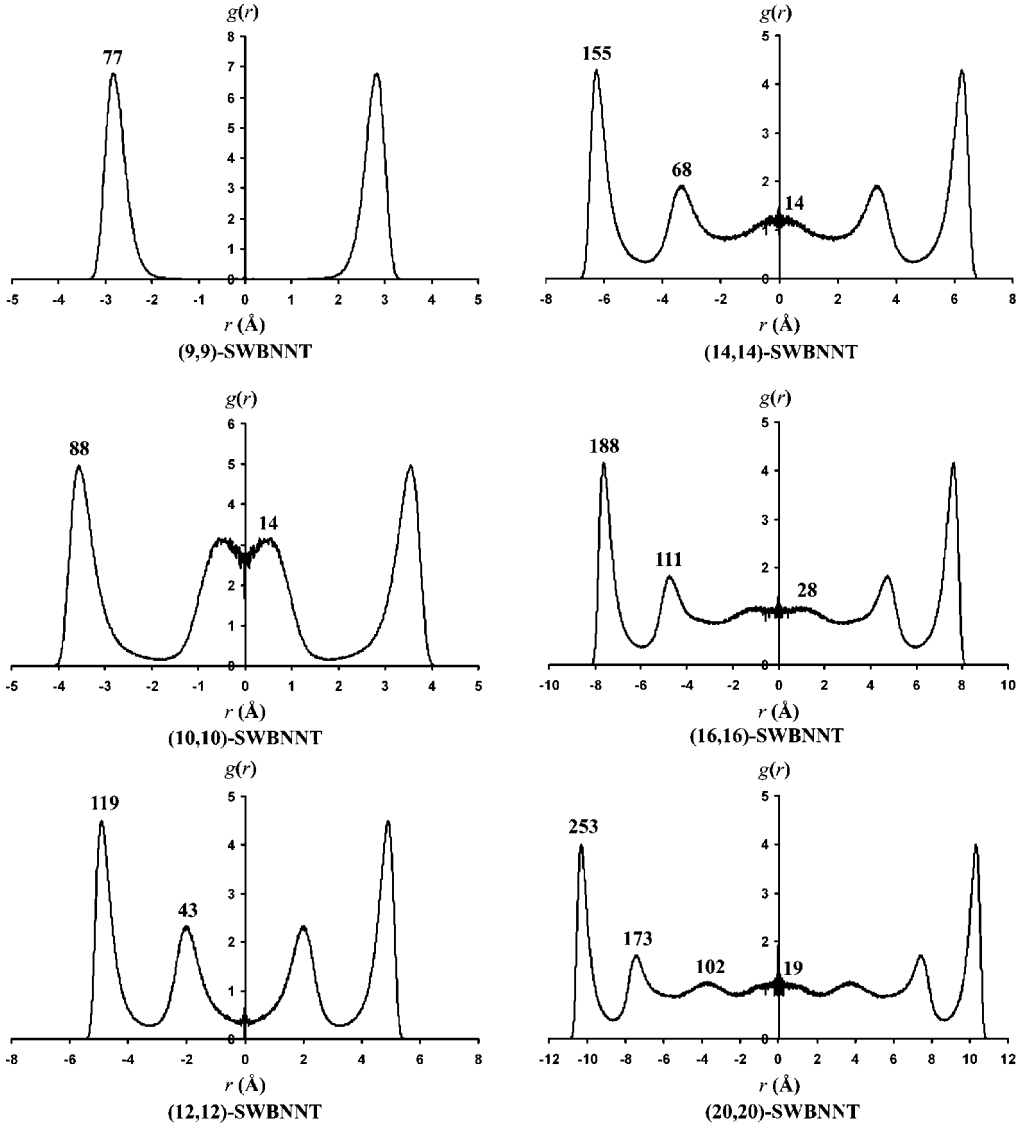

Figure 1. Local density distribution functions, in cylindrical coordinates, for the water molecules in the SWBNNTs. The numbers above the curves indicate the number of molecules present, on the average, in the various regions.

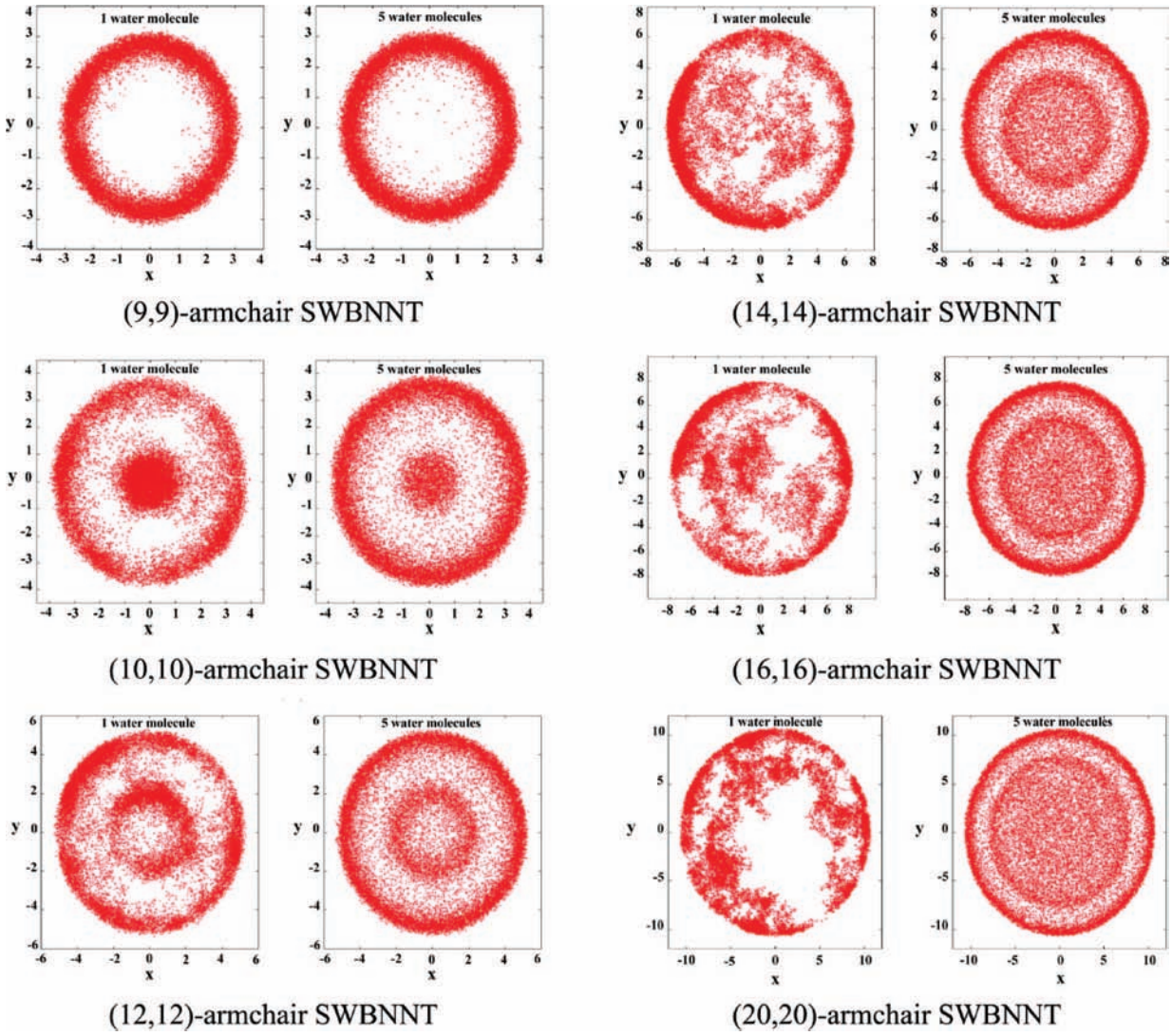

Figure 2. Trajectories of 1 (left) and 5 (right) arbitrarily selected water molecules in the SWBNNTs, corresponding to Figure 1, monitored during 1 ns. Note that the scale is not the same for all tubes.

lattice, where $\mathbf{a}_1$ and $\mathbf{a}_2$ are unit vectors. These nanotubes are filled with a total number of 77, 102, 162, 237, 327, and 547 water molecules, respectively, which leads to an average water density of 1.0 g/cm^3 in the tube.

Water is described by the extended simple point charge (SPC/E) model ($\varepsilon_{O-O} = 0.1554$ kcal/mol and $\sigma_{O-O} = 3.16$ Å).[21,22] The geometry of each water molecule is kept rigid using the SHAKE algorithm. The two hydrogen atoms are located at 1.0 Å from the oxygen with an H−O−H angle of 109.5°. Atomic charges of $-0.8476e$ and $+0.4238e$ are assigned to the oxygen and hydrogen sites, respectively.

The interactions between water and the nanotube wall are described by a 12-6 LJ potential. The LJ parameters for carbon ($\varepsilon_{C-C} = 0.0970$ kcal mol^{-1} and $\sigma_{C-C} = 3.36$ Å) are taken from ref 14. The water−nanotube interaction parameters are derived by using the Lorentz−Berthelot combining rules i.e., $\varepsilon_{ij} = (\varepsilon_i\varepsilon_j)^{1/2}$ and $\sigma_{ij} = (\sigma_i + \sigma_j)/2$, where ε_{ij} and σ_{ij} symbolize the strength and size of the LJ potential parameters between sites i and j.

The degree of "nanotube hydrophobicity" is varied for all tubes by changing the strength of the LJ potential parameter (ε_{O-C}) between water and wall as an independent parameter, keeping the size parameter (σ_{C-C}) unchanged. Hydrophobicity is said to increase when ε_{O-C} is reduced. We study the case $\varepsilon_{O-C} = 0.1143$ kcal/mol, a 7% reduction compared to the full value $\varepsilon_{O-C} = 0.1230$ kcal/mol. These simulations are labeled a, e.g. (9,9)-SWCNTa; simulations with the full potential are labeled b. Furthermore, we study a case which models boron nitride nanotubes (SWBNNT) isostructural to the carbon tubes. Still keeping the σ-value constant, we set $\varepsilon = 0.1216$ and 0.1502 kcal/mol for the oxygen−boron and oxygen−nitrogen interactions, respectively, as in ref 11. Already the 7% decrease in hydrophobicity is found to lead to a loss of water conductivity in the small (5,5)-SWCNT.[11] Similarly, it is found that in (5,5)-armchair SWBNNT attractive interactions between water and nitrogen sites are primarily accountable for the good water conduction. Therefore, it seemed interesting to look at the diffusion and structural properties of water confined in large diameter tubes also of this type. Further details of the nanotube-simulations are given in Table 1. A pure SPC/E-water box at 298 K was also run for comparison.

The coordinates for the wall atoms of the nanotubes are generated by using the Materials Studio Visualizer program.[23] Short pieces of tube are then surrounded by about 2,000 SPC/E water molecules in a simulation box, *NpT* simulations are started with $p = 1$ atm and the temperature is lowered from high values to $T = 298$ K. In a few 10 ps, depending on tube size, the small sections of the tubes are filled with water. Several of these

pieces, for details see below, are then put together in a periodic box and equilibrated before starting the production runs.

All MD production simulations are performed in the canonical (*NVT*) ensemble at a temperature of 298 K using the Nosé-Hoover thermostat implemented in the DL_POLY program package,[24] version 2.17. The dimensions of the periodic simulation box for each system are twice the nanotube diameter in the *x*- and *y*-directions and the length of the tube in the *z*-direction. The principal axis of the nanotube is the *z*-axis of the simulation box. Periodic boundary conditions are applied to all three directions. The long-range electrostatic interactions between water molecules are computed using the Ewald method, and the short-range van der Waals interactions are computed up to a cutoff radius equal to the nanotube diameter for $m = 9$, 10, and 12, and equal to 18.44 Å for $m = 14$, 16, and 20. The equations of motion are integrated with a 0.25-fs time step. The production runs are conducted for at least 1 ns following the equilibration period of 0.25 ns. During the production runs, the coordinates and velocities are stored, usually every 50 fs, for further analyses.

III. Results and Discussion

(a) Structure. Figure 1 shows the so-called cylindrical $g(r)$-functions across the boron-nitride nanotubes. The numbers above the curves refer to the average number of water molecules present in the various regions; the total number of molecules is listed in Table 1. In the (9,9) case only one peak appears, in keeping with the results by Mashl et al.[14] for their (9,9) single-wall nanotube, while starting from the (10,10) and in the larger tubes, the cylindrical RDF shows two peaks indicating layering. The distance between these two peaks is 2.89, 2.89, 2.91 and 2.92 Å in the (12,12), (14,14), (16,16), and (20,20) tubes, respectively, larger than the r_{OO} distance of the first maximum of the $g(r_{OO})$-function in bulk water (2.76 Å). In the tubes with diameters above 18 Å the water density at the interior layer is very close to bulk density; inside a cylinder of 2.2 Å radius around the *z*-axis of the (20,20) tube it is exactly 1.0 g/cm^3.

Figure 2 gives a visual impression of the water arrangements (and motions) by showing the *x*- and *y*-coordinates of one (left) and five (right) arbitrarily selected water molecules plotted at regular time intervals during the simulations. The functions for the other two cases, SWCNTa and SWCNTb, are very similar to Figures 1 and 2 and are, therefore, not shown here. The boundary-layer peaks are only slightly enhanced with increasing wall−water interactions, as expected. As an example, we find an average of 250, 252, and 253 water molecules in the boundary layer in the cases of (20,20) SWCNTa, SWCNTb, and SWBNNT, respectively. The motions of the water molecules will be analyzed below.

When water molecules are confined in nanotubes, their neighborhoods differ from those in the bulk phase. A molecule is said here to have *n* neighbors if at a given time there are simultaneously *n* oxygen atoms with distances of r_{OO} < the first minimum of the bulk $g(r_{OO})$ (i.e., 3.33 Å) from the central oxygen atom. This definition does of course not imply that the coordination of the central oxygen is necessarily tetrahedral. Figure 3 shows the distributions of the number of neighbors, as defined above, for the SWBNNTs, separately for water molecules in the center and near the wall of the tubes, and in pure water. In the (9,9) tube all water molecules are located close to the wall and there is no water in the center of the pore, see Figures 1 and 2. The water structure in this tube is indeed peculiar with an extremely strong preference for four neighbors. For the wider nanotubes, a regular pattern emerges with a more

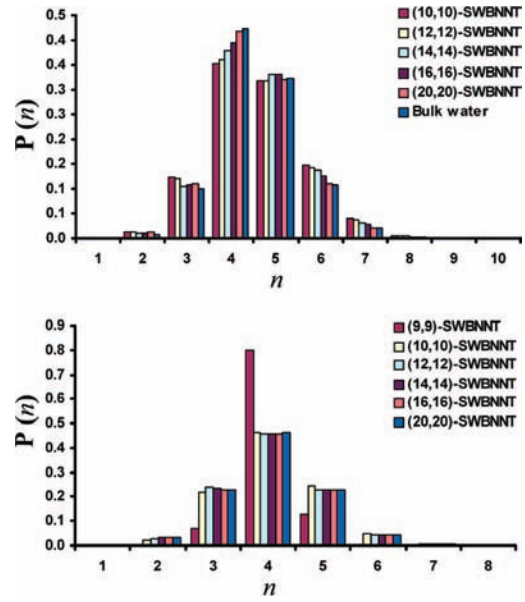

Figure 3. Distributions of the number of water neighbors of a water molecule in the interior (top) and in the outermost layer (bottom) in SWBNNT and, for comparison, in pure SPC/E water (top).

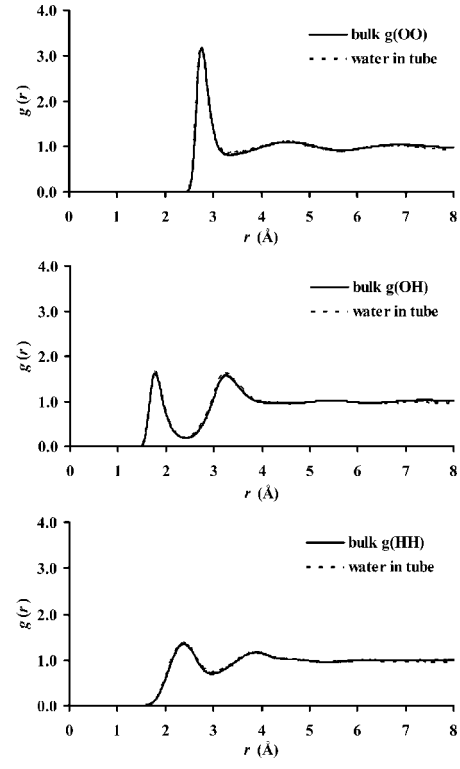

Figure 4. Radial distribution functions g_{OO}, g_{OH}, and g_{HH} for pure water (solid) and for water molecules in the center (−2.2 Å < r < 2.2 Å) of the (20,20) SWBNNT (dashed).

or less invariable distribution of neighbors in the outermost layer and distributions in the interior converging with increasing tube diameter toward the one for pure water.

In order to further analyze the water structure in the center of a large tube, Figure 4 compares the three radial distribution functions (rdf) $g(r_{OO})$, $g(r_{OH})$, and $g(r_{HH})$ obtained in our pure bulk water reference run (see Table 1) with the ones obtained for molecules in the center of the (20,20) SWBNNT. Only sites inside a cylinder of 2.2 Å radius around the *z*-axis (see Figure 1) are selected as centers for this function. Since the number

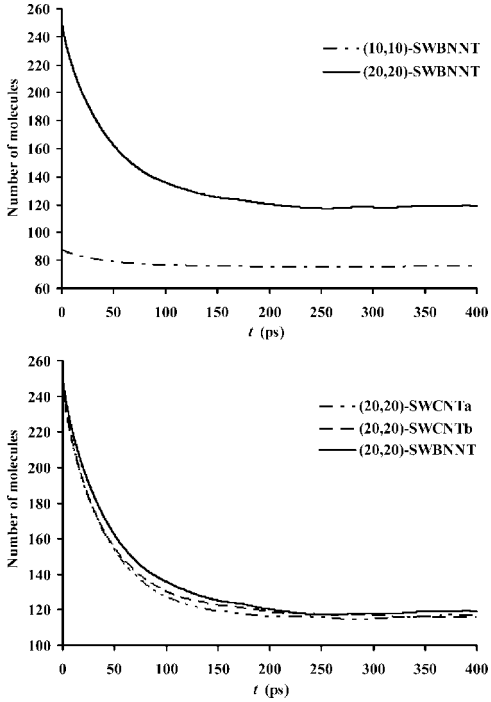

Figure 5. Average number of water molecules present in the outermost water layer at time 0 and still present there at later times, from simulation of (10,10) and (20,20) SWBNNT (top), and additionally, for comparison, for SWCNTa and SWCNTb (bottom).

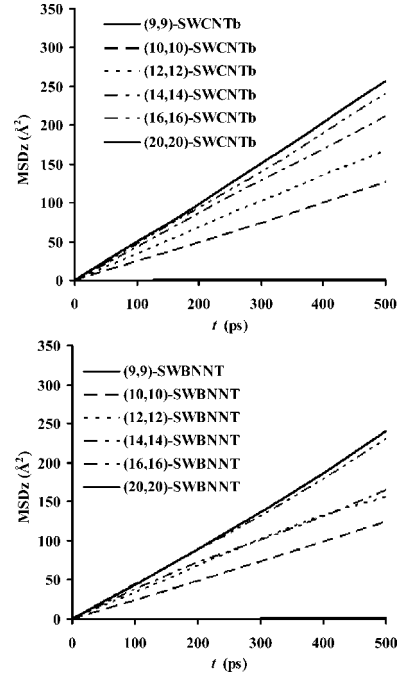

Figure 6. Mean square displacements of the oxygen atoms of water in the SWCNTbs (top) and SWBNNTs (bottom). For the self-diffusion coefficients, see Table 2 and Figure 7.

density is not constant across the tube, the normalization of these functions is somewhat arbitrary. The zone of roughly constant density inside the tube is about 8-Å wide, we thus selected to set $g(r \approx 6\ \text{Å}) = 1$ to ease comparisons. The figure shows that the three g-functions inside the tube are almost indistinguishable from the bulk ones. Thus, even with the strongest of our three wall−water interaction models, the water inside the larger tubes is, at least as far as the radial structure is concerned, very close to bulk water.

(b) Dynamics. Figure 5 shows the decay of the number of water molecules present in the boundary layer of the tube wall [defined as the water molecules with $r = \sqrt{(x^2 + y^2)}$ values larger than the minima in the distribution functions shown in Figure 1] at an initial time t_0, as a function of time. This figure shows, as examples, the results for a large and a small tube and also for a large tube with different interactions strengths (hydrophobicities) between water and wall. They confirm the visual impression obtained from Figure 2, namely that a given water molecules samples more or less the entire tube interior during the duration of our simulations.

The long time limit of these correlation functions is the expectation value of the initial molecules being present in the boundary layer when the system is totally mixed. It is seen that this value is reached, within the fluctuations, in all cases after about 150 ps. Functions of type

$$f(t) = a + b \cdot \exp(-t/\tau) \tag{1}$$

describe the correlation very well in all cases; the correlation times τ are all between 40 and 50 ps with the higher values for the stronger wall−water interactions. The sum $a + b$ obtained from the fits is, as it should be, close to the average total number of water molecules present in the boundary layer, which is also reported in Figure 1 from integrations of the distribution functions plotted there.

Figure 6 shows the averaged mean-square displacements of the oxygen atoms of the water molecules, corrected for the random drifts induced by the thermostat. The translational self-diffusion coefficients reported in Table 2 and Figure 7 have been obtained by fitting expressions

$$\left\langle (z - z_0)^2(t) \right\rangle = A + 2D_z t \tag{2}$$

to the mean-square displacement curves in z-direction at long times. We obtained a value of $D = 2.5 \pm 0.1 \times 10^{-5}$ cm^{2}s^{-1} from our pure water simulation. This D-value is intermediate between the values reported by Mashl[14] (2.69×10^{-5} cm^{2}s^{-1}) and by experimental diffusion coefficient of water (2.30×10^{-5} cm^2 s^{-1}).[25] In passing, we also take good note of the remarks in these papers that the fact that the experimental D is well reproduced by a given model for the pure liquid at a given state point does not necessarily mean that it will also do so in solutions, at an interface, or under different thermodynamic conditions. We nevertheless expect systematic trends (e.g., size dependences, or when the wall−water interactions are modified) to be reasonably well mirrored.

Figure 7 shows that no self-diffusion can be detected in the narrowest tubes during our simulation runs of a few nanoseconds. D_z increases with increasing tube diameter and comes close to its bulk value in our widest tubes with diameters of about 24 Å, the convergence toward this value being faster for smaller wall−water interactions. In the case of the boron-nitride tubes the convergence is not monotonous. We were not able to pinpoint the particular structural features that may explain the plateau in D_z observed between the (10,10) and (14,14) tubes (which we think is outside our uncertainties) in a convincing way. Even larger irregular variations of the self-diffusion have been observed by Mashl et al.[14] in narrower CNTs. No influence of the wall−water interactions can be distinguished in tubes wider than about 20 Å.

It is seen in Figure 6 that the linear regime of the mean-square displacement is reached typically after about 10 ps. Comparing this time with the typical time for water molecules to stay in the boundary layer discussed above (viz. 40 to 50 ps, see Figure 5), indicates that a separation of the total self-

TABLE 2: Axial Self-Diffusion Coefficients D_z ($cm^2\ s^{-1}$) of Water in Nanotubes at the Average Temperature of 298 K and the Water Density of 1.0 g/cm^3[a]

model	D_z ($cm^2\ s^{-1}$)	model	D_z ($cm^2\ s^{-1}$)	model	D_z ($cm^2\ s^{-1}$)
bulk water	2.50×10^{-5}				
(9,9)-SWCNTa	3.00×10^{-8}	(9,9)-SWCNTb	9.80×10^{-8}	(9,9)-SWBNNT	8.60×10^{-8}
(10,10)-SWCNTa	1.20×10^{-5}	(10,10)-SWCNTb	1.30×10^{-5}	(10,10)-SWBNNT	1.20×10^{-5}
(12,12)-SWCNTa	2.00×10^{-5}	(12,12)-SWCNTb	1.70×10^{-5}	(12,12)-SWBNNT	1.60×10^{-5}
(14,14)-SWCNTa	2.30×10^{-5}	(14,14)-SWCNTb	2.10×10^{-5}	(14,14)-SWBNNT	1.60×10^{-5}
(16,16)-SWCNTa	2.40×10^{-5}	(16,16)-SWCNTb	2.40×10^{-5}	(16,16)-SWBNNT	2.40×10^{-5}
(20,20)-SWCNTa	2.70×10^{-5}	(20,20)-SWCNTb	2.60×10^{-5}	(20,20)-SWBNNT	2.50×10^{-5}

[a] The uncertainties are estimated to be of the order of $\pm 0.1 \times 10^{-5}$ $cm^2\ s^{-1}$.

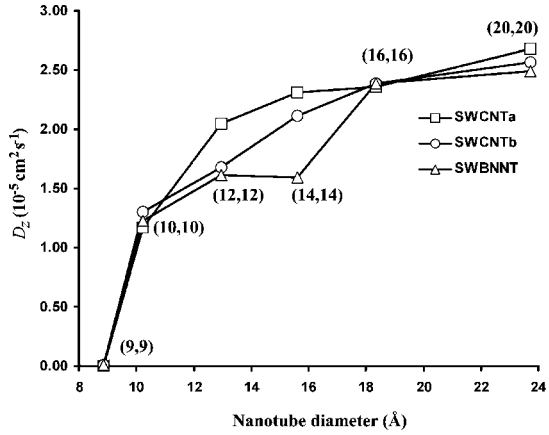

Figure 7. Axial self-diffusion coefficients D_z (10^{-5} $cm^2\ s^{-1}$) of water in nanotubes as a function of tube size.

diffusion into a component originating in the boundary layer molecules and a second one originating in the bulk would be justified. This work is presently ongoing.

IV. Summary and Conclusions

Molecular dynamics computer simulations at room temperature of water-filled single-wall model nanotubes with diameters ranging from about 9 Å to about 24 Å have shown that, by and large, the influence of the wall on the local density of the water and on its self-diffusion does not extend much beyond the layer of molecules directly adsorbed to the wall. In particular circumstances, probably when the geometrical constraints by and the interactions with the wall favor the formation of particular water structures, anomalies cannot be ruled out even in tubes of intermediate widths.

Varying the strength of the wall−water interactions within reasonable limits for carbon or boron-nitride tubes does not alter these conclusions. The adsorbed water layer, on the other hand, is very strongly affected both in its structure and in its dynamics. The characteristic time for the exchange dynamics between the adsorbed layer and the rest of the water is of the order of about 40 to 50 ps, i.e. relatively long compared to the time needed for the diffusive regime to be reached in normal, unconfined water at the same thermodynamic conditions.

Acknowledgment. This work was supported in part by Grants from the Thailand Research Fund (to J.L. and P.A.B.) and the Kasetsart University Research and Development Institute (KURDI), the National Nanotechnology Center (NANOTEC Center of Excellence and CNC Consortium), the National Research Council of Thailand (NRCT), and the Commission on Higher Education (Postgraduate Education and Research Programs in Petroleum and Petrochemicals, and Advanced Materials to J.L. as well as Postdoctoral Research Scholar to T.N.). The support from the Graduate School Kasetsart University (to N.A.) is also acknowledged.

References and Notes

(1) O'Connell, M. J. *Carbon Nanotubes: Properties and Applications*; CRC Press: Boca Raton, FL, 2006.
(2) Iijima, S. *Nature* **1991**, *354*, 56–58.
(3) Wang, Z. L.; Poncharal, P.; De Heer, W. A. *J. Phys. Chem. Solids* **2000**, *61*, 1025–1030.
(4) Sui, H.; Han, B. G.; Lee, J. K.; Walian, P.; Jap, B. K. *Nature* **2001**, *414*, 872–878.
(5) Kolesnikov, A. I.; Zanotti, J.-M.; Loong, C.-K.; Thiyagarajan, P.; Moravsky, A. P.; O. Loutfy, R. O.; Burnham, C. J. *Phys. Rev. Lett.* **2004**, *93*, 035503/1–035503/4.
(6) Chou, C.-C.; Hsiao, H.-Y.; Hong, Q.-S.; Chen, C.-H.; Peng, Y.-W.; Chen, H.-W.; Yang, P.-C. *Nano Lett.* **2008**, *8*, 437–445.
(7) Tajkhorshid, E.; Nollert, P.; Jensen Morten, O.; Miercke Larry, J. W.; O'Connell, J.; Stroud Robert, M.; Schulten, K. *Science (New York)* **2002**, *296*, 525–530.
(8) Bianco, A.; Kostarelos, K.; Prato, M. *Curr. Opin. Chem. Biol.* **2005**, *9*, 674–679.
(9) Hummer, G.; Rasaiah, J. C.; Noworyta, J. P. *Nature* **2001**, *414*, 188–190.
(10) Waghe, A.; Rasaiah, J. C.; Hummer, G. *J. Chem. Phys.* **2002**, *117*, 10789–10795.
(11) Won, C. Y.; Aluru, N. R. *J. Am. Chem. Soc.* **2007**, *129*, 2748–2749.
(12) Beckstein, O.; Biggin, P. C.; Sansom, M. S. P. *J. Phys. Chem. B* **2001**, *105*, 12902–12905.
(13) Allen, R.; Hansen, J.-P.; Melchionna, S. *J. Chem. Phys.* **2003**, *119*, 3905–3919.
(14) Mashl, R. J.; Joseph, S.; Aluru, N. R.; Jakobsson, E. *Nano Lett.* **2003**, *3*, 589–592.
(15) Liu, Y.; Wang, Q.; Wu, T.; Zhang, L. *J. Chem. Phys.* **2005**, *123*, 234701–234707.
(16) Koga, K.; Tanaka, H.; Zeng, X. C. *Nature* **2000**, *408*, 564–567.
(17) Liu, Y.; Wang, Q. *Phys. Rev.* **2005**, *72*, 085420/1–085420/4.
(18) Liu, Y.; Wang, Q.; Zhang, L.; Wu, T. *Langmuir* **2005**, *21*, 12025–12030.
(19) Joseph, S.; Aluru, N. R. *Nano Lett.* **2008**, *8*, 452–458.
(20) Won, C. Y.; Aluru, N. R. *J. Phys. Chem. C* **2008**, *12*, 1812–1818.
(21) Berendsen, H. J. C.; Grigera, J. R.; Straatsma, T. P. *J. Phys. Chem.* **1987**, *91*, 6269–6271.
(22) Guillot, B. *J. Mol. Liq.* **2002**, *101*, 219–260.
(23) Accelrys, Inc. *Materials Studio, 4.2 V*; Accelrys, Inc.: San Diego, CA, 2007.
(24) Smith, W.; Forester, T. R.; Todorov, I. T.; Leslie, M. *The DL_POLY 2.0, User Manual, Version 2.17*; CCLRC, Daresbury Laboratory: Daresbury, U.K., 2006.
(25) Price, W. S.; Ide, H.; Arata, Y. *J. Phys. Chem. A* **1999**, *103*, 448–450.

JP8088676